Efficient *In Vivo* T_2 Mapping by Prior-information-driven SLIM-BLAST Reconstruction

Jeffrey TSAO[1], Victor D. SCHEPKIN[1], Paul C. LAUTERBUR[1]

[1]Biomedical Magnetic Resonance Laboratory, University of Illinois at Urbana-Champaign, 2100 S. Goodwin Ave., Urbana, IL USA;

Introduction

A number of methods have been proposed to speed up T_2 mapping (1-3). The common approach is to reduce the number of sampled points along the relaxation curve. In the case of mono-exponential decay, two images at different echo times provide sufficient data to determine the T_2 decay and the scaling constant on a pixel-by-pixel basis. In this study, we propose a more efficient way of T_2 mapping by taking advantage of the correlations among nearby pixels. We show that such prior information can be used to reduce the data requirement substantially. A new reconstruction algorithm is proposed, which is capable of obtaining *in vivo* mono-exponential T_2 maps using data from only one and a quarter images. The new algorithm is called SLIM-BLAST. "SLIM" stands for Signal Localization by IMaging (4), and "BLAST" stands for Broad-use Linear Acquisition Speed-up Technique (5).

Theory

Mono-exponential T_2 maps were created from the ratio between an early- and a late-echo image. The early-echo image was obtained by acquiring 100% of its *k*-space data and applying inverse Fourier transform. It was then used as prior information to reconstruct the late-echo image, for which only 25% of the phase encode lines were used. The reconstruction of the late-echo image involved 4 steps:

1. Inverse Fourier transform: The frequency encoding direction was reconstructed conventionally, by inverse Fourier transform. Then, each image column along the phase encoding direction was reconstructed separately in subsequent steps.

2. SLIM step: For each image column along the phase encoding direction, the early-echo image was divided into a small number of segments. The late-echo image was then approximated as a linear combination of these segments using SLIM (4). The SLIM equations were solved using Truncated Singular Value Decomposition (TSVD), with the condition number kept below 50 to prevent excessive noise amplification. Segmentation of the early-echo image was performed by an automatic algorithm, which iteratively selected the most prominent intensity edges until there were 6 segments per image column. All background and bone segments (as identified by intensity thresholding) were counted as a single non-contiguous segment, as were all fat and marrow segments.

3. BLAST step: BLAST (5) is based on the Generalized Series model (6). It models the reconstructed image $\rho(x)$ as:

$$\rho(x) = R_{static}(x) + (R_{dynamic}(x) + \lambda) \times \sum c_i \exp(-2\pi \times k_i)$$

where $R_{static}(x)$, $R_{dynamic}(x)$, λ, and c_i represent the static reference image, the dynamic reference image, regularizer, and basis coefficients, respectively. In the present case, $R_{static}(x)$ was chosen to be the reconstructed image from SLIM. $R_{dynamic}(x)$ was used to highlight regions where the SLIM reconstruction might differ from the true image. In general, most of the SLIM reconstruction errors were located at tissue boundaries, due to inaccuracies in segmentation. Therefore, $R_{dynamic}(x)$ was chosen to be the gradient magnitude of the early-echo image, normalized to 1. λ was set empirically to 1%. In general, the value of λ could be chosen from the data by cross validation (7), albeit at the expense of increased computation. The basis coefficients c_i were determined by fitting the above equation to the measured *k*-space data. The solution was obtained by TSVD with the condition number kept below 15.

4. Filtering and data consistency: The effect of the above reconstruction steps was to extrapolate data in the unmeasured portion of *k*-space. As with any extrapolation, the extrapolated data become more error-prone as one moves farther from the measured portion of *k*-space. This error was reduced by gradually tapering the extrapolated data to zero towards the outer edges of *k*-space with a Hamming filter. Data consistency was enforced by replacing the measured portion of *k*-space with the actual measured data.

Methods

Axial images were acquired from the lower legs of 5 human subjects. For each subject, seven 256×128 (frequency × phase) spin-echo images were acquired with TR=600ms and TE=24, 27, 32, 38, 44, 51, and 60ms in randomized order. The images were first reconstructed by inverse Fourier transform using the full data set. A gold-standard T_2 map was created from these images by mono-exponential fitting. Then, a second T_2 map was created with the SLIM-BLAST procedure as described above, using 100% data of the 24ms TE image (128 phase encodes) and only 25% data of the 60ms TE image (32 phase encodes, from *k*-space position –8 to 23). The two T_2 maps were compared for consistency.

Results & Discussion

Typical results are shown in the figure. The top shows the gold-standard T_2 map derived from Fourier reconstruction using data from 7 images. The bottom shows the T_2 map derived from SLIM-BLAST reconstruction using reduced data acquisition. There was a slight loss in resolution for the SLIM-BLAST reconstruction, but the overall features were well preserved. Some spurious black and white specks were visible in both T_2 maps, and they were caused by flow artifacts and slight subject motion during acquisition. Excluding these spurious pixels and low-intensity pixels (i.e. background and bone), the mean and median absolute difference in T_2 values between the Fourier and SLIM-BLAST reconstructions were less than 4ms and 3ms, respectively, in all 5 subjects.

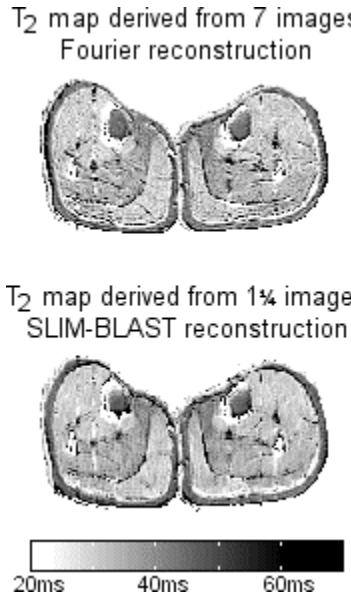

SLIM-BLAST is a general method for improving the time efficiency of image acquisition. It is a data-consistent method, so its reconstruction is guaranteed to approach the Fourier reconstruction as the number of phase encodes increases. SLIM-BLAST can be combined with fast acquisition pulse sequences to further improve T_2 mapping speed. This capability may prove important for studying the rapid dynamics of T_2 changes, such as in muscles during exercise (8).

Acknowledgments

Many thanks to Drs. Zhi-Pei Liang, Yoram Bresler, and Joan Dawson for valuable discussions, and to Ms. Sherrie Frydenger for her technical assistance. This work was supported by grants PHS 5 P41 RR05964 and PHS RO1 CA 51430.

References

1. Deichmann R *et al. MRI* 13:633-639. 1995. **2.** McKenzie CA *et al. MRM* 41:208-212. 1999. **3.** Does MD *et al. JMR* 147:116-120. 2000. **4.** Hu X *et al. MRM* 8: 314-22, 1988. **5.** Tsao J *et al. ISMRM* 2001. **6.** Liang ZP *et al. IEEE-TMI* 10: 132-137, 1991. **7.** Golub GH *et al. Technometrics* 21:215-223. 1979. **8.** Fisher M *et al. Invest Radiol* 25: 480-485. 1990.